ApJ, to be submitted

Formation of hard very-high energy spectra of blazars in leptonic models

E. Lefa[1,2]

[1] *Max-Planck-Institut für Kernphysik, P.O. Box 103980, 69029 Heidelberg, Germany*

[2] *Landessternwarte, Königstuhl 12, 69117 Heidelberg, Germany*

eva.lefa@mpi-hd.mpg.de

F.M. Rieger[1]

[1] *Max-Planck-Institut für Kernphysik, P.O. Box 103980, 69029 Heidelberg, Germany*

and

F. Aharonian[1,3]

[1] *Max-Planck-Institut für Kernphysik, P.O. Box 103980, 69029 Heidelberg, Germany*

[3] *Dublin Institute for Advanced Studies, 31 Fitzwilliam Place, Dublin 2, Ireland*

ABSTRACT

The very high energy (VHE) γ-ray spectra of some TeV Blazars, after being corrected for absorption in the extragalactic background light (EBL), appear unusually hard, which poses challenges to conventional acceleration and emission models. We investigate the parameter space that allows the production of such hard TeV spectra within time-dependent leptonic models, both for synchrotron self-Compton (SSC) and external Compton (EC) scenarios. In the context of interpretation of very hard γ-ray spectra, time-dependent considerations become crucial because even extremely hard, initial electron distributions can be significantly deformed due to radiative energy losses. We show that very steep VHE spectra can be avoided if adiabatic losses are taken into account. Another way to keep extremely hard electron distributions in the presence of radiative losses, is to assume stochastic acceleration models that naturally lead to steady-state relativistic, Maxwellian-type particle distributions. We demonstrate that in either case leptonic models can reproduce TeV spectra as hard as $E_\gamma\ dN/dE_\gamma \propto E_\gamma$. Unfortunately this limits, to a large extend, the potential of extracting EBL from γ-ray observations of blazars.

Subject headings: BL Lacertae objects: general – diffuse radiation – gamma-rays: observations – gamma-rays: theory.

1. Introduction

Blazars constitute a sub-class of Active Galactic Nuclei (AGN) characterized by broad-band (from radio to VHE γ-rays), non-thermal emission produced in relativistic jets pointing close to the line of sight to the observer (Urry & Padovani 1995). The highly variable luminosity of Blazars (which often exhibits 2 peaks) are commonly interpreted in terms of a synchrotron-inverse Compton origin.

In synchrotron self-Compton (SSC) models, the X-ray emission is usually attributed to the synchrotron radiation of relativistic electrons. The Compton up-scattering of these synchrotron photons by the same electron population then produces the high energy γ-ray radiation (e.g., Maraschi et al. 1992; Bloom & Marcher 1996). Under specific circumstances, the target radiation field for inverse Compton upscattering can be dominated by external photons, leading to so-called external Compton (EC) models (e.g., Dermer et al. 1993; Sikora et al. 1994). In general, these leptonic models have been relatively successful in describing the observed SED of Blazars.

The recent detections of VHE γ-rays from Blazars with redshift $z \geq 0.1$ (in particular, 1ES 1101-232 at $z = 0.186$ and 1ES 0229+200 at $z = 0.139$), however, poses challenges to the conventional leptonic interpretation. VHE γ-rays emitted by such distant objects arrive after significant absorption caused by their interactions with extragalactic background light (EBL) via the process $\gamma\gamma \rightarrow e^+e^-$ (e.g., Gould & Schréder 1967). Reconstruction of the absorption-corrected intrinsic VHE γ-ray spectra based on state-of-the-art EBL models then yields unusually hard VHE source spectra, that are difficult to account for with standard inverse Compton assumption.

One characteristic case concerns the distant (at $z = 0.186$) Blazar 1ES 1101-232, detected at VHE γ-ray energies by the H.E.S.S. array of Cherenkov telescopes (Aharonian et al. 2006, 2007a). When corrected for absorption by the EBL, the VHE γ-ray data result in very hard intrinsic spectra, with a peak in the SED above 3 TeV and a photon index $\Gamma \leq 1.5$. A similar behavior has also been detected in the TeV Blazar 1ES 0229+200 (at z=0.139) (Aharonian et al. 2007b). Though there is a non-negligible uncertainty in the EBL flux, the intrinsic spectra are unusually hard even when one considers the lowest levels of the EBL (Franceschini et al. 2008). Other models predicting higher EBL flux would lead to even harder (intrinsic) photon indices close to 1 (e.g., Stecker & Scully 2008). We note that a

recent analysis of Fermi LAT data for the nearby TeV Blazar Mkn 501 indicates a hard γ-ray spectrum (Γ close to 1) at lower (10-200 GeV) energies (Neronov et al. 2011). If confirmed, this would be strong evidence for unusually hard γ-ray spectra independent of questions related to the level of EBL. On the other hand and apart from the challenges arising for inverse Compton interpretations, the observed hard VHE spectra obviously carry important information about the level of the EBL, and thus a deep understanding of the mechanisms acting within these sources becomes now even more critical.

The "simplest" way to overcome the problem is to assume that there is no absorption. In fact, this is possible in Lorentz invariance violation scenarios (Kifune 1999). We should note however that this effect is likely to be true only above 2 TeV (Stecker & Glashow 2001), whereas the hard spectra problem we face in the case of distant Blazars is relevant to sub-TeV energies as well. Another non-standard mechanism to avoid severe absorption in the EBL has been suggested by De Angelis et al. 2009 who proposed that γ-ray photons could oscillate into a new very light axion-like particle close enough to the source and be converted back before reaching the Earth. To some extend a similar idea was recently suggested by Essey et al. 2011 who suggested that the γ-rays from Blazars may be dominated by secondary γ-rays produced along the line of sight by the interactions of cosmic rays protons with background photons. While the first scenario would require the existence of exotic particles, the second needs extraordinary low magnetic fields of the order of $10^{-15}G$.

In more standard-type astrophysical scenarios, the formation of hard γ-ray spectra is related to the production and absorption processes. Photon-photon absorption could in principle result in arbitrarily hard spectra provided that the γ-rays pass through a hot photon gas with a narrow distribution such that $E_\gamma \epsilon_o >> m_e c^2$. In this case, due to the reduction of the cross-section, the source becomes optically thick at lower energies and thin at higher energies, thus leading to formation of hard intrinsic spectra. (Aharonian et al. 2008; Zacharopoulou et al. 2011)

If one relates the hard γ-ray spectra to the production process, then this implies correspondingly hard parent particle distributions. Outside standard leptonic models, a number of alternative explanations have been explored in the literature. In analogy to pulsar winds, Aharonian et al. (2002) for example have analyzed the implications of a cold ultra-relativistic outflow that initially (close to the black hole) propagates at very high speeds. In such a case, up-scattering of ambient photons can yield sharp pile-up features in the intrinsic source spectra. However, very high bulk Lorentz factors would be needed ($\Gamma_b \sim 10^7$) and it seems not clear whether such a scenario can be applied to Blazars. On the other hand, if Blazar jets would remain highly relativistic out to kpc-scales ($\Gamma_b \sim 10$) and able to accelerate particles, a hard (slowly variable) VHE emission component could perhaps be produced by Compton

up-scattering of CMB photons (Böttcher et al. 2008).

In order to produce hard γ-ray spectra within standard leptonic, synchrotron-inverse Compton scenarios, hard electron energy distributions are required. Although standard shock acceleration theories, both in the non-relativistic and relativistic regime, predict quite broad, $n(E) \propto E^{-2}$-type, electron energy distributions, there are non-conventional realizations which could give rise to very hard spectra (Derishev et al. 2003; Stecker et al. 2007). On a more phenomenological level, Katarzyński et al. (2007) have shown that the presence of an energetic power-law electron distribution with a high value of the minimum cut-off energy can lead to a hard TeV spectrum. In general, however, injection of a hard electron distribution is not a sufficient condition as electrons are expected to quickly lose their energy due to radiative cooling and thereby develop a standard $n(E) \propto E^{-2}$ form below the initial cut-off energy. In order to avoid synchrotron cooling, one thus needs to assume unusually small values for the magnetic field within the source (Tavecchio et al. 2009).

To some extent, this situation can be avoided if one invokes adiabatic losses. This is demonstrated below by means of a time-dependent investigation assuming dominant adiabatic energy losses. As a second alternative, we discuss pile-up (Maxwellian-type) electron distributions, that can be formed in stochastic acceleration scenarios. As these distributions are steady-state solutions with radiative (synchrotron or Thomson) losses already included, there is no need to avoid these losses. Maxwellian-type electron distributions provide an interesting explanation for the very hard TeV components as their radiation spectra share many characteristics with the (hardest possible) mono-energetic distributions.

It is obviously important to explore the strengths and limitations of such explanations in more details, both theoretically and observationally, in order to understand whether there is a need to invoke more exotic scenarios.

In the present work we explore the conditions under which a narrow, energetic particle distribution is able to successfully account for the hard VHE source spectra. To this end, we examine different electron distributions within the context of standard leptonic models, i.e. the one-zone SSC and the external Compton scenario. The paper is structured as following: The requirements for quasi-stationary SSC solutions are analyzed in Sect. 2. Apart from narrow, power-law-type electron distributions, quasi-Maxwellian distributions are examined. A time-dependent generalization including adiabatic losses is explored in Sect. 3. Section 4 discusses the possibilities within an external Compton approach.

2. Stationary SSC with an energetic electron distribution

Within a stationary SSC approach, the hardest possible (extended) VHE spectrum is approximately $F_\nu \propto \nu^{1/3}$, where $F_\nu = dF/d\nu$ is the spectral flux (differential flux per frequency band). This has a simple explanation: The emitted synchrotron spectrum of a single electron with Lorentz factor γ in a magnetic field B, averaged over the particle's orbit, obeys $j(\nu,\gamma) \propto G(x)$, where $G(x)$ is a dimensionless function with $x = \nu/\nu_c$ and $\nu_c \equiv 3\gamma^2 eB\sin\alpha/(4\pi m_e c)$. For $x \ll 1$, the functional dependence of $G(x)$ is well approximated by $G(x) \propto x^{1/3}$, while for $x \gg 1$ one has $G(x) \propto x^{1/2}e^{-x}$ (e.g., Rybicki & Lightman 1979). Hence, at low frequencies $\nu \ll \nu_c$, the synchrotron spectrum follows $j(\nu) \propto \nu^{1/3}$. Compton up-scattering of such a photon spectrum in the Thomson regime by a very energetic, narrow electron distribution will preserve this dependence and therefore yield a VHE spectral wing as hard as $F_\nu \propto \nu^{1/3}$ (see below).

2.1. Power-law electron distribution with high low-energy cut-off

A homogeneous SSC scenario with a high value for the low-energy cut-off of the non-thermal electron distribution has consequently been proposed by Katarzyński et al. (2007) to overcome the problem of the Klein-Nishina (KN) suppression of the cross-section at high energies and to reproduce VHE spectra as hard as 1/3. Let us assume that the electron population follows a power-law distribution of index p between the low- and high-energy cut-offs

$$N'_e(\gamma') = K'_e\gamma'^{-p}, \quad \gamma'_{\rm min} < \gamma' < \gamma'_{\rm max}\,, \tag{1}$$

as often used in modeling the Blazar spectra. Here, prime quantities refer to the blob rest frame and unprimed to the observer's frame. Taking relativistic Doppler boosting (δ) into account, the observed synchrotron flux from an optically thin source at distance d_L is given by the integral of $N'_e(\gamma')d\gamma'$ times the single particle emissivity $j'(\nu',\gamma')$ over the volume element and all energies γ' (e.g., Begelman et al. 1984), i.e

$$F_\nu^{\rm syn} = \frac{\delta^3}{d_L^2}\int_{V'}\int_{\gamma'} j'(\nu',\gamma')N'_e(\gamma')d\gamma' dV'\,. \tag{2}$$

The above expression yields the common power-law of index $\alpha = (p-1)/2$ between the frequency limits $\nu_{\rm min} \propto \delta(B\gamma^2_{\rm min})$ and $\nu_{\rm max} \propto \delta(B\gamma^2_{\rm max})$. Below and above those limits, the electrons with energy around the minimum and maximum cut-off dominate, and thus the spectrum approximately exhibits a slope $F_\nu \propto \nu^{1/3}$ for $\nu < \nu_{\rm min}$, and an exponential cut-off

for $\nu > \nu_{max}$, i.e.

$$F_\nu \propto \begin{cases} \nu^{1/3}, & \nu << \nu_{min} \\ \nu^{-\frac{p-1}{2}}, & \nu_{min} \leq \nu \leq \nu_{max} \\ \nu^{1/2} e^{-\nu}, & \nu >> \nu_{max} \end{cases} \quad (3)$$

The hard 1/3-slope appears in the VHE range of EC γ-rays when the synchrotron photons are up-scattered to higher energies by the electron population given by equation (1) with a high $\gamma_{\rm min}$ and provided that the Thomson regime applies. Obviously, it will be significantly softer in the KN regime. In any case, however, there exists a characteristic energy below which the Compton spectrum mimics the behavior of the synchrotron spectrum $F_\nu \propto \nu^{1/3}$.

Note that the inverse Compton-scattered spectrum of a monochromatic photon field by mono-energetic electrons approximately follows, at low up-scattered photon energies, $F_\nu \propto \nu$ (cf. Blumenthal & Gould 1970). Thus, any photon field which is softer (flatter) than $F_\nu \propto \nu$ will dominate the lower-energy part of the up-scattered emission and thus, in the standard SSC scenario the 1/3-VHE slope (the 4/3-slope in the νF_ν representation) is the hardest that can be achieved.

An exemption to this may occur if the magnetic field in the source would be fully turbulent with zero mean component. In such a case, the low-frequency part of the synchrotron spectrum could be harder than $F_\nu \propto \nu^{1/3}$ (Medvedev 2006; Derishev 2007; Reville & Kirk 2010), which will then be reflected to low-energy part of the Compton component.

The "critical Compton energy" is usually $\epsilon_{\rm min} \simeq \delta\gamma_{\rm min}^2(b\gamma_{\rm min}^2)$, where $b \equiv (B/B_{cr})m_e c^2$, $B_{cr} = m_e^2 c^3/(e\hbar)$, except when the deep KN regime applies, i.e., when up-scattering of the minimum synchrotron photons by the minimum energy electrons occurs in the KN regime so that $\frac{4}{3}b\gamma_{\rm min}^3 > 1$. If the latter applies, then the corresponding energy below which one can see the hard 1/3-slope is, as expected, $\gamma_{\rm min} m_e c^2$, and it approximately corresponds to the peak of the emitted luminosity for any power-law electron index (see Fig. 1). In the KN regime, the peak appears especially sharp (e.g., Tavecchio et al. 1998), and the Compton flux has a strong inverse dependence on the value of $\gamma_{\rm min}$. For example, for the realization presented in Fig. (1), the emissivity in this regime roughly scales as $j^C \propto \gamma_{\rm min}^{-2.5}$, so that slight changes in $\gamma_{\rm min}$ can lead to significant variations in the amplitude of the Compton peak flux. On the other hand, as long as $p < 3$ (positive synchrotron slope in a νF_ν representation) the synchrotron peak luminosity would remain approximately constant.

A power-law electron distribution with a high low-energy cutoff has been used in Tavecchio et al. (2009) in order to reproduce the SED of the blazar 1ES 0229+200 within a stationary SSC approach. The high value of $\gamma_{\rm min} \sim 10^5$ then ensures the hard Compton part of the spec-

trum with 1/3-slope is in the TeV range. The generic difficulty for such an approach is that an energetic electron distribution is expected to quickly develop a γ^{-2}-tail below $\gamma_{\rm min}$ due to synchrotron cooling, thereby making the Compton VHE spectrum softer (see Fig. 2). To overcome this problem, Tavecchio et al. (2009) suggested an unusually low value for the magnetic field, $B \sim (10^{-4} - 10^{-3})$ G, that would allow the electron distribution to remain essentially unchanged on timescales of up to a few years. Obviously, one would then not expect to observe significant variability on shorter timescales. We note however, that this requirement could be relaxed if one assumes that the detected γ-ray signal is a superposition of short flares which can not be detected individually. Arguments based on magnetic flux conservation naively suggest that the magnetic field value, when scaled from the black hole region to the emission site, should be at least one or two orders of magnitude higher so that one would need to destroy magnetic flux for such a scenario to work. On the other hand, a narrow but very energetic electron distribution in combination with such low magnetic field strengths implies a strong deviation from equipartition, thereby obviously facilitating an expansion of the source.

2.2. Relativistic Maxwellian electron distribution

As far as a narrow energetic particle distribution is concerned, a relativistic Maxwellian may come as a more natural representation. Such an electron distribution can be the outcome of a stochastic acceleration process (e.g., 2nd order Fermi) that is balanced by synchrotron (and/or Compton) energy losses, or in general any energy loss mechanism that exhibits a quadratic dependence on the particle energy (see e.g., Schlickeiser 1985; Aharonian et al. 1986; Henri & Pelletier 1991; Stawarz & Petrosian 2008).

Consider for illustration the Fokker-Planck diffusion equation which describes the stationary distribution function $f(p)$ of electrons that are being accelerated by, e.g., scattering off randomly moving Alfvén waves in an isotropic turbulent medium,

$$\frac{1}{p^2}\frac{\partial}{\partial p}\left(p^2 D_p \frac{\partial f(p)}{\partial p}\right) + \frac{1}{p^2}\frac{\partial}{\partial p}\left(\beta_s p^4 f(p)\right) = 0\,, \tag{4}$$

where D_p is the momentum-space diffusion coefficient. Particle escape is neglected in eq. (4), as the timescale for synchrotron cooling is expected to be much smaller than the one for electron escape.

For scattering off Alfvén waves, one has $D_p = \frac{p^2}{3\tau}(\frac{V_A}{c})^2 \equiv D_0 p^{2-\alpha_p}$, with $V_A = \frac{B}{\sqrt{4\pi\rho}}$ the Alfvén speed and $\tau = \lambda/c \propto p^{\alpha_p}$, $\alpha_p \geq 0$, the mean scattering time (e.g., Rieger et al. 2007). If the turbulent wave spectrum $W(k) \propto k^{-q}$ is assumed to be Kolmogorov-type

($q \simeq 5/3$) or Kraichnan-type($q = 3/2$), the momentum-dependence becomes $\alpha_p = 1/3$ and $\alpha_p = 1/2$, respectively. Bohm-type diffusion, on the other hand, would imply $\alpha_p = 1$, while hard-sphere scattering is described by $\alpha_p = 0$. Note, however, that if one considers electron acceleration by resonant Langmuir waves, even $D_p = \text{const}$ ($\alpha_p = 2$) may become possible (Aharonian et al. 1986).

The synchrotron energy losses that appear in the second term of Eq. (4) are

$$\frac{dp}{dt} = -\beta_s p^2 = -\frac{4}{3}(\sigma_T/m_e^2c^2)U_B p^2 \tag{5}$$

In the γ-parameter space, the solution of Eq. (4) becomes a relativistic Maxwell-like function

$$f(\gamma) = A\gamma^2 e^{-\left(\frac{\gamma}{\gamma_c}\right)^{1+\alpha_p}}\,, \tag{6}$$

($\alpha_p \neq -1$) with

$$\gamma_c = \left(\frac{[1+\alpha_p]D_0}{\beta_s}\right)^{1/(1+\alpha_p)} (m_e c^2)^{-1}\,, \tag{7}$$

and constant A to be defined by the initial conditions. Note that this is a steady-state solution already including radiative losses and there is no need to invoke extreme values for the magnetic field. The critical Lorentz factor γ_c approximately corresponds to the energy at which acceleration on timescale

$$t_{\rm acc} = \frac{3}{4-\alpha_p}\left(\frac{c}{V_A}\right)^2 \tau \tag{8}$$

is balanced by (synchrotron) cooling on timescale $t_{\rm cool} = 1/[\beta_s p]$. Depending on the choice of parameters, a relatively large range of values for γ_c is possible and thus, cut-off energies of the order of $\gamma_c \sim 10^5$ may well be achieved. Consider, for example, Bohm-type diffusion with $\tau = \eta r_g/c$, $r_g = \gamma m_e c^2/(eB)$ the electron gyro-radius and $\eta \geq 1$. Using $t_{\rm acc} = t_{\rm cool}$, the maximum electron Lorentz factor becomes $\gamma_c \simeq 10^6\ (v_A/0.01c)\ (1\ {\rm G}/B)^{1/2}\eta^{-1/2}$.

The synchrotron spectrum that arises from a Maxwell-like electron distribution is dominated by the emission of electrons with γ_c (Fig. 3). It exhibits the characteristic 1/3-slope up to the corresponding "synchrotron cut-off frequency" $h\nu_c^{\rm syn} \sim \delta b \gamma_c^2$ where $b = B/B_{cr}$ and $B_{cr} = m^2c^3/e\hbar$. Thus the Compton spectrum is very similar to the one resulting from a narrow power-law if one chooses a value for the cut-off energy close to the minimum electron energy of the power-law distribution. The peak of the Compton flux then contains information for the cut-off energy as $\nu^c_{\rm peak} \propto \gamma_c$.

Note that for an electron distribution of the form of eq. (6) that exhibits an exponential cutoff $\propto \exp[-(\gamma/\gamma_c)^\beta]$, the corresponding cut-off in the synchrotron spectrum appears much

smoother, $\propto \exp[-(\nu/\nu_*)^{\beta/(\beta+2)}]$ (Fritz 1989; Zirakashvili & Aharonian 2007). The position of the synchrotron peak flux, ν_p, is then also dependent on β, and one can show that for $\beta = 1$ (or $\alpha_p = 0$ in the previous notation) an important factor ~ 10 arises, so that $\nu_p = 9.5\nu_c$, whereas for $\beta = 3$ the synchrotron peak corresponds approximately to the electron cut-off as $\nu_p = 1.2\nu_c$ (e.g., Fig. 3).

3. Time-dependent case - expansion of the source

Expansion of the source could change the conclusions drawn above. In particular, if one assumes a very low magnetic field such that synchrotron losses are negligible, then adiabatic losses may become important and alter the electron distribution. In this section, we examine the behavior of the system for a power-law electron distribution with a high value of the low-energy cut-off discussed above. For simplicity, we consider a spherical source that expands with a constant velocity u,

$$R(t) = R_0 + u(t - t_0)\,. \tag{9}$$

The relativistic electron population will be affected by synchrotron losses,

$$P_{\rm syn} = -\frac{d\gamma}{dt} = \frac{\sigma_T B(t)^2 \gamma^2}{6\pi m_e c}\,, \tag{10}$$

and by adiabatic losses (e.g., Longair 1982),

$$P_{\rm ad} = -\frac{d\gamma}{dt} \simeq \frac{1}{3}\frac{\dot{V}}{V}\gamma = \frac{\dot{R}(t)}{R(t)}\,\gamma = \frac{u}{R(t)}\,\gamma\,. \tag{11}$$

As the emission region expands, the magnetic field decreases. We consider a scaling $B \propto (1/R)^m \propto (1/t)^m$ with $1 \leq m \leq 2$ to study the evolution of the system. The limiting value $m = 2$ corresponds to conservation of magnetic flux for the longitudinal component, whereas $m = 1$ holds for the perpendicular component. (Note that for $m = 1$ the ratio of the electrons' energy density to the magnetic field energy density remains constant). Which energy loss process then determines the electron behavior depends mainly on the magnetic field strength and the size of the source. A simple comparison of the above relations shows that when $P_{\rm ad} > P_{\rm syn}$, i.e.,

$$B(t)^2 R(t) < \frac{6\pi m_e c^2}{\sigma_T}\left(\frac{u}{c}\right)\frac{1}{\gamma} = 2.3\times 10^{19}\left(\frac{u}{c}\right)\frac{1}{\gamma} \tag{12}$$

adiabatic losses dominate over radiative losses. For example, if one considers expansion at speed $u \sim c$ and an initial source dimension $R_0 \sim 10^{14}$ cm, then for energies below $\gamma \sim 10^7$ the magnetic field can be as large as $B \sim 0.1$ G and for energies less than $\gamma \sim 10^5$ the

adiabatic losses are still dominant for a value of $B \sim 1$ G. If the expansion of the source would not affect the hard slope at TeV energies, this could thus allow for a relaxation of the values used for SSC modeling of the source. In order to investigate this scenario in more detail, one needs to solve the electrons' kinetic equation

$$\frac{\partial N_e(\gamma,t)}{\partial t} = \frac{\partial}{\partial \gamma}\left(P_{\rm ad} N_e(\gamma,t)\right) - \frac{N_e(\gamma,t)}{\tau_e} + Q(\gamma,t)\,, \tag{13}$$

where τ_e is the characteristic escape time and N_e the differential electron number. For simplicity, we neglect the escape term ($\tau_e \to \infty$), assuming that the sources expands with relativistic speeds $u \sim 0.1$c. For a constant expansion rate and continuous injection with rate $Q(\gamma,t) \to Q(\gamma,R)$, we can replace the time variable t by the source dimension R. Then, the general solution of the kinetic equation (eq. (30) in Atoyan & Aharonian 1999) for the case of dominance of adiabatic losses is reduced to

$$N_e(\gamma,R) = \frac{R}{R_0}\, N_0\left(\frac{R}{R_0}\gamma\right) + \frac{1}{u}\int_{R_0}^{R} \frac{R}{r}\, Q\left(\frac{R}{r}\gamma, r\right) dr\,, \tag{14}$$

where the first term corresponds to the initial conditions, the contributions of which quickly disappears, and the second term relates to the continuous injection of relativistic electrons. R_0 is the source dimension at the initial time t_0.

We consider zero initial conditions ($N_0 = 0$) and power-law injection of relativistic particles at constant rate

$$Q(\gamma,R) = Q_0 \gamma^{-p_1}\, \Theta(\gamma - \gamma_{0,\rm min})\Theta(\gamma_{0,\rm max} - \gamma)\Theta(R - R_0)\,, \tag{15}$$

where Θ denotes the unit step function

$$\Theta(x - x_0) = \begin{cases} 1, & x > x_0 \\ 0, & x < x_0\,, \end{cases} \tag{16}$$

$p_1 > 0$ is the momentum index and R_0 the radius at which injection starts. At radius R, electrons with initial cut-off energies $\gamma_{0,\rm max}$ and $\gamma_{0,\rm max}$ will have energies $\gamma_{R,\rm min}$ and $\gamma_{R,\rm max}$, respectively, as they evolve according to Eq. (11), i.e. we have

$$\gamma_R = \gamma_0 \frac{R_0}{R(t)} \propto \frac{1}{t}\,. \tag{17}$$

Moreover, there exists a critical radius $R_* = R_0 \gamma_{0,\rm max}/\gamma_{0,\rm min}$ at which $\gamma_{R,\rm max}$, i.e. the energy of the electron with initial injected energy $\gamma_{0,\rm max}$ at R, becomes less than the initial $\gamma_{0,\rm min}$, so that the following two cases can be distinguished:

For $R < R_*$, or equivalently as long as $\gamma_{\rm R,max} > \gamma_{0,\rm min}$, we have

$$N(\gamma,R) = \frac{Q_0}{p_1 u} R \begin{cases} \gamma^{-p_1}\left[1-\left(\frac{\gamma}{\gamma_{0,\rm max}}\right)^{p_1}\right], & \gamma_{\rm R,max} < \gamma < \gamma_{0,\rm max} \\ \gamma^{-p_1}\left[1-\left(\frac{R_0}{R}\right)^{p_1}\right], & \gamma_{0,\rm min} < \gamma < \gamma_{\rm R,max} \\ \gamma_{0,\rm min}^{-p_1} - \left(\frac{R\gamma}{R_0}\right)^{-p_1}, & \gamma_{\rm R,min} < \gamma < \gamma_{0,\rm min} \end{cases} \tag{18}$$

For $R > R_*$, or equivalently as long as $\gamma_{\rm R,max} < \gamma_{0,\rm min}$, the solution is

$$N(\gamma,R) = \frac{Q_0}{p_1 u} R \begin{cases} \gamma^{-p_1}\left[1-\left(\frac{\gamma}{\gamma_{0,max}}\right)^{p_1}\right], & \gamma_{0,min} < \gamma < \gamma_{0,\rm max} \\ \gamma_{0,\rm min}^{-p_1} - \gamma_{0,\rm max}^{-p_1}, & \gamma_{\rm R,max} < \gamma < \gamma_{0,\rm min} \\ \gamma_{0,\rm min}^{-p_1} - \left(\frac{R\gamma}{R_0}\right)^{-p_1}, & \gamma_{\rm R,min} < \gamma < \gamma_{\rm R,max} \end{cases} \tag{19}$$

The two solutions exhibit the same behavior. The differential electron number density drops with radius as $n_e(\gamma,R) = \frac{N_e(\gamma,R)}{\rm Volume} \propto R^{-2}$, and above the initial low-energy cut-off $\gamma_{0,\rm min}$ adiabatic losses do not modify the power-law index $n_e(\gamma,t) \propto \gamma^{-p_1}$ (Kardashev 1962). Below $\gamma_{0,\rm min}$ the resulting distribution is constant with respect to the electron energies, $n_e(\gamma,R) \propto \gamma^0$ (Fig. 4). The γ^0-part of the electron population does not show up in the spectrum as the contribution of the injected $\gamma_{0,\rm min}$ electrons (generating a 1/3-synchrotron wing) remains dominant at low energies (Figs. 5 and 6). Thus, in contrast to the simple synchrotron cooling case, one has $F_\nu \propto \nu^{1/3}$ below the injected cut-off. For this reason, the classical hard spectrum picture at the TeV range can remain for timescales analogous to the source size. Even though electrons cool adiabatically as the source expands, the hard 1/3-synchrotron slope always appears below the synchrotron frequency related to the initial minimum Lorentz factor

$$\nu_{\rm min}^{\rm syn} \propto \gamma_{0,\rm min}^2 B(R) \propto \frac{1}{t^m}\,. \tag{20}$$

Note that any decrease of this break energy occurs due to a decrease of the magnetic field. This is different to the pure synchrotron cooling case, where the corresponding break energy follows the evolution of the minimum electron energy so that $\nu_{\rm min}^{\rm syn} \propto 1/t^2$. The same consideration holds for the energy regime where Compton scattering occurs. When we are deep in the KN regime ($b(R)\gamma_{0,\rm min}^3 > 1$) the energy below which the hard slope remains is, as mentioned above,

$$\nu_{\rm min}^{C} \propto \gamma_{0,\rm min}\,. \tag{21}$$

It therefore does not move to lower energies though the corresponding synchrotron frequency does. (In the pure synchrotron cooling case, obviously, $\nu^C_{\rm min} \propto 1/t^2$). As the source expands and the magnetic field drops, there will be an instant t corresponding to a radius R at which the KN regime no longer applies, and the break Compton frequency becomes

$$\nu^C_{\rm min} \propto B(R)\gamma^4_{0,\rm min} \propto \frac{1}{t^m}\,, \tag{22}$$

which now moves to lower frequencies with the same rate as the synchrotron one. (Note that this reveals a very different time-dependence compared to the pure synchrotron cooling case where now $\nu^C_{\rm min} \propto 1/t^4$). However, the peak of the Compton flux still remains close to the initial $\gamma_{0,\rm min}$ energy (Fig. 7), and in total the decrease of the synchrotron peak flux is much stronger than the decrease in the Compton peak flux (Fig. 8). In general, the dependence of the magnetic field on the radius R has important consequences for the behavior of the system even though the synchrotron losses are not important. The synchrotron peak flux varies as

$$F^{syn}_\nu \propto N_e B(R)^2 \tag{23}$$

and as we know from the solution of the kinetic equation that $N_e \propto R$, the variability of the synchrotron luminosity should reflect the magnetic field dependence. The Compton flux, on the other hand, does not necessarily vary quadratically with respect to the synchrotron flux. As discussed above, the drop of the minimum Compton energy (which occurs naturally within the expansion-scenario) reduces the suppression of the cross-section and thereby supports the Compton emission. The variability pattern after "saturation" can therefore approach a quasi-linear dependence (cf. Fig 8). Initially, during the raising phase before the two luminosities reach their maximum, the Compton flux can vary much more strongly, almost more than quadratically, with respect to the synchrotron flux. Moreover, close to saturation the Compton luminosity can exhibit a delay with respect to the synchrotron one as it reaches its maximum at later times compared to the synchrotron luminosity.

The above considerations apply to situations where the expansion of the source completely determines the evolution of the system. In reality, synchrotron losses could modify the electron distribution at high energies, namely for

$$\gamma > \gamma_* = \frac{6\pi m_e c^2}{\sigma_T R B(R)^2}\left(\frac{u}{c}\right)\,. \tag{24}$$

However, as synchrotron losses decrease faster than adiabatic losses, one only needs to ensure that initially $\gamma_* > \gamma_{0,\rm min}$. The change of the electron power index from $-p_1$ to $-p_1-1$ due to synchrotron cooling (cooling break) above $\gamma_{0,\rm min}$ would then not disturb the hard 1/3 slope in the TeV range.

4. The external Compton case

An alternative hypothesis to the SSC scenario concerns the Comptonization of a radiation field external to the electron source. In general, the optical-UV radiation field produced by a standard accretion disk could represent a non-negligible external source of photons to be up-scattered to the VHE γ-ray part of the spectrum. This radiation field could be up-scattered either directly by the relativistic electrons of the jet (with target photons coming directly from the accretion disk, Dermer et al. 1993) or more effectively after being reprocessed/re-scattered by emission line clouds like the broad line region (BLR) (Sikora et al. 1994). In external Compton (EC) scenarios, the geometry of the source and the location of the photon field with respect to the jet are of high importance as they can result in strong boosting or de-boosting effects on the photon energies. Here we explore the possibility of producing a hard TeV spectrum within the EC approach. We consider the BLR case, where the photon field is strongly boosted in the frame of the jet and up-scattered to higher energies.

Let us consider a blob of relativistic electrons that travels with the jet of bulk Lorentz factor Γ along the z-axis. The jet passes through a region assumed to be filled with isotropic and homogeneous photons that obey a Planckian distribution of temperature $T \sim 10^4 - 10^5 K$ (corresponding peak frequency $\nu_d = 2.82kT/h \sim 5 \times 10^{14} - 10^{15}$ Hz). The central disk photon field is then characterized by a special intensity

$$I_\nu^d = \frac{2h\nu^3}{c^2(e^{\frac{h\nu}{kT}} - 1)}\,, \tag{25}$$

a fraction $\xi < 1$ of which we assume is isotropized by re-scattering or reprocessing in the BLR (Sikora et al. 2002), so that the spectral energy density of the target photon field is

$$U_\nu^{\rm BLR} = \frac{\xi L_\nu^d}{4\pi c r_{\rm BLR}^2}\,, \tag{26}$$

where $L_\nu^d = 4\pi^2 r_d^2 I_\nu^d$ is the spectral luminosity of the disk and where we take $r_d \sim r_s$ for the disk radius.

In order to take anisotropic effects into account, we transform the electron distribution from the comoving blob frame K' to the rest frame K of the external photon field, which in our case coincides with the observer's frame (Georganopoulos et al. 2001). Electrons are assumed to be isotropic in the blob frame K'. In the photon frame K they exhibit a strong dependence on the angle θ, which is the observer's angle. As the up-scattered photons travel inside a cone $1/\gamma$, we can make the approximation that they follow the direction of the electrons. The angle between the electron momentum and the bulk velocity of the

jet coincides with the observer's angle. The observer practically sees radiation only from electrons that in the photon frame are directed towards him. The observed flux then is

$$F_{\epsilon_\gamma} = \frac{\delta^3}{d_L^2} \int N'_e(\frac{E}{\delta})\ W(E, \epsilon_{\rm ph}, \epsilon_\gamma)\ n_{\rm ph}(\epsilon_{\rm ph}) dE\ d\epsilon_{\rm ph} \tag{27}$$

where $N_e(E)$ denotes the differential number of electrons per energy per solid angle, and $W = E_\gamma \frac{dN}{dtdE_\gamma}$ is the scattered photon spectrum per electron (given in Blumenthal & Gould 1970). The unprimed quantities refer to the external photon field frame with number density $n_{\rm ph}(\epsilon_{\rm ph})$ and the primed ones to the blob rest frame.

We show the calculated Compton spectrum for a Maxwellian electron distribution in Fig. 9. The resulting TeV slope appears even harder than in the SSC case, with a limiting value of $F_\nu \propto \nu^1$. Any photon field which is softer (flatter) than $F_\nu \propto \nu^1$ will dominate the Compton spectrum at low energies, as in our SSC model case where the up-scattered (synchrotron) photon spectrum follows $F_\nu \propto \nu^{1/3}$. In all other cases, like in the external Compton scenario with a Planckian photon field (that at low energies follows $F_\nu \propto \nu^2$), the characteristic behavior of the Compton cross-section appears, implying that the Compton spectrum at low energies (i.e., below $\sim \gamma_c^2 \epsilon_c$, where γ_c is the electron break frequency in the photon rest frame) is dominated by the contribution from the up-scattering of the peak photons with $\epsilon_c \sim 3kT$, yielding a $F_\nu \propto \nu$ dependence.

A similar consideration holds for a narrow (energetic) power-law electron distribution in an expanding source scenario. A hard VHE component $F_\nu \propto \nu$ should then appear below $\delta\gamma_{0,\rm min}$. The critical energy below which one can see this hard behavior of the Compton flux will not move to lower energies as the external target photon field is quasi-stable, so that the condition for the deep Klein-Nishina regime $\gamma_{0,\rm min}\epsilon_c > 1$ does not change.

5. Summary

The observed hard γ-ray spectra of TeV Blazars are difficult to explain within the most popular leptonic synchrotron-Compton models. The $n(E) \propto E^{-2}$ shape, that the electron energy distribution is expected to quickly develop due to synchrotron cooling, usually results in a $F_\nu \propto \nu^{-1/2}$ radiation spectrum and therefore represents the limiting value of how hard the up-scattered spectrum can be in the TeV range. Moreover, modification due to Klein-Nishina effects can make the up-scattered TeV spectrum steeper than this and shift the Compton peak to much lower energies than observed.

However, intrinsic source spectra as hard as $F_\nu \propto \nu^{-1/2}$ exist, even when one only corrects for the lowest level of the EBL, most notably in the case of 1ES 1101-232 and

1ES 0229+200 (Aharonian et al. 2006, 2007b). Most likely, the real source spectra are even harder. Investigating the possibility of forming hard VHE blazar spectra appears therefore particularly important. Methodologically, it seems necessary to first examine the "conventional" radiation and acceleration mechanisms, that have often been successful in interpreting Blazar observations, before adopting very different and often more extreme solutions.

The results of this work show that within a simple homogeneous one-zone SSC approach, a power-law particle distribution with a large low-energy cutoff can in principle produce a hard ($\alpha = 1/3$) – slope in the VHE domain ($F_\nu \propto \nu^\alpha$) by reflecting the characteristic low-energy slope of the single particle synchrotron spectrum (cf. also Katarzyński et al. 2007). As shown in section 4, even harder VHE spectra approaching $F_\nu \propto \nu$ ($\alpha = 1$) can be achieved in the external Compton case for a Planckian-type ambient photon field.

A power-law electron distribution with a high low-energy cut-off has been used in Tavecchio et al. (2009) to model the emission from 1ES 0229+200 within a stationary SSC approach. In order to avoid the above noted synchrotron cooling problem, an unusually low value for the magnetic field strength was employed, leaving the particle distribution essentially unchanged on the timescales of several years. This goes along with a strong deviation from simple equipartition by several orders of magnitude (i.e., $u_B/u_e \lesssim 10^{-5}$). While it is known from detailed spectral and temporal SSC studies of the prominent γ-ray Blazar Mkn 501 that TeV sources may be out of equipartition at the one per-mill level or less (Krawczynski et al. 2002), the SSC modeling of 1ES 0229+200 suggest the hard spectrum sources to belong to the more extreme end. (Within external Compton models values closer to equipartition may be achieved, depending on the external photon field energy density). On the other hand, a large electron energy density (strongly exceeding the magnetic field one) could well facilitate an expansion of the source, and this motivates a time-dependent analysis:

Using a time-dependent SSC model, we have shown that the hard ($\alpha = 1/3$)-VHE slope can be recovered, when adiabatic losses dominate over the synchrotron losses for the low-energy part of the electron distribution (i.e., for Lorentz factors less than the injected $\gamma_{\rm min}$). The main reason for this is, that the resultant electron distribution below $\gamma_{\rm min}$ becomes flat and therefore does not show up in the SSC spectrum. Interestingly, this scheme also allows one to relax the very low magnetic field constraints.

We also examined the relevance of a Maxwellian-like electron distribution that peaks at high electron Lorentz factors $\sim 10^5$. Such a distribution represents a simple time-dependent solution that already takes radiative energy losses into account, and turns out to be capable of successfully reproducing the hard spectra in the TeV range (with limiting values $\alpha = 1/3$ and $\alpha = 1$, respectively). Maxwellian distributions can be the outcome of a stochastic

acceleration process balanced by synchrotron or Thomson cooling. Depending on the physical conditions within a source, e.g., if particles undergo additional cooling in an area different from the acceleration one (Saugé & Henri 2006; Giebels et al. 2007), or if the medium is clumpy supporting a "multi-blob" scenario in which the observed radiation is the result of superposition of regions characterized by different parameters, the combination of pile-up distributions may allow a suitable interpretation of different type of sources. For the case presented here, they demonstrate a physical way of achieving the high low-energy cut-offs needed in leptonic synchrotron-Compton models for the hard spectrum sources.

Although our main purpose here is not to fit data, Fig. 10 shows that a Maxwellian-type electron distribution could also provide a satisfactory explanation for the hard TeV component in 1ES 0229+200.

Our results illustrate that even within a leptonic synchrotron-Compton approach relatively hard intrinsic TeV source spectra may be encountered under a variety of conditions. While this may be reassuring, the possibility of having such hard source spectra within "standard models" unfortunately constrain the potential of extracting limits on the EBL density based on γ-ray observations of Blazars, one of the hot topics currently discussed in the context of next generation VHE instruments.

Acknowledgement: We would like to thank S. Kelner and S. Wagner for helpful discussions.

REFERENCES

Aharonian, F.A., Atoyan, A. M., & Nahapetian, A. 1986, A&A, 162, L1

Aharonian, F.A., Timokhin, A.N., & Plyasheshnikov, A.V. 2002, A&A, 384, 834

Aharonian, F., et al. 2006, Nature, 440, 1081

Aharonian, F., et al., 2007a, A&A, 470, 475

Aharonian, F., et al., 2007b, A&A, 475, L9

Aharonian, F.A., Khangulyan, D., & Costamante, L. 2008, MNRAS, 387, 1206

Atoyan A. M., & Aharonian F. A. 1999, MNRAS, 302, 253

Begelman, M.C., Blandford, R.D., & Rees, M.J. 1984, Reviews of Modern Physics, 56, 255

Bloom, S.D. & Marscher A.P. 1996, ApJ, 461, 657

Blumenthal, G.R. & Gould, R.J. 1970, Reviews of Modern Physics, 42, 237

Böttcher, M., Dermer, C.D., & Finke, J.D. 2008, ApJ, 679, L9

De Angelis, A., Mansutti, O., Persic, M., & Roncadelli, M. 2009, MNRAS, 394, L21

Derishev, E. V. 2007, Ap&SS, 309, 157

Derishev, E.V., Aharonian, F.A., Kocharovsky, V.V., Kocharovsky, Vl. V. 2003, Phys. Rev. D, 68, 043003

Dermer C.D., & Schlickeiser R. 1993, ApJ, 416, 458

Essey, W., Kalashev, O., Kusenko, A., & Beacom, J. F. 2011 ApJ, 731 51E

Franceschini, A., Rodigliero, G., & Vaccari, M. 2008, A&A, 487, 837

Fritz, K.D. 1989, A&A, 214, 14

Georganopoulos, M., Kirk, J.G., & Mastichiadis, A. 2001, ApJ, 561, 111

Giebels, B., Dubus, G., & Khélifi, B. 2007, A&A, 462, 29

Gould, R.J., & Schreder, G.P. 1967, Physical Review, 155, 1408

Henri, G., & Pelletier, G. 1991, ApJL, 383, L7

Kardashev, N. S. 1962, Soviet Astronomy, 6, 317

Katarzyński, K., Ghisellini, G., Tavecchio, F., Gracia, J., & Maraschi, L. 2006, MNRAS, 368, L52

Kifune, T. 1999, ApJL, 518, L21

Krawczynski, H., Coppi, C.S., & Aharonian, F. 2002, MNRAS, 336, 721

Maraschi, L., Ghisellini, G., & Celotti, A. 1992, ApJL, 397, L5

Medvedev, M. V. 2006, ApJ, 637, 869

Neronov, A., Semikoz, D. & A.M. Taylor 2011, A&A submitted (arXiv:1104.2801)

Reville, B., & Kirk, J. G. 2010, ApJ, 724, 1283

Rieger, F.M., Bosch-Ramon, V., & Duffy, P. 2007, Ap&SS, 309, 119

Rybicki, G.B., & Lightman, A.P. 1979, Radiative Processes in Astrophysics, Wiley, New York

Saugé, L., & Henri, G. 2006, A&A, 454, L1

Schlickeiser, R. 1985, A&A, 143, 431

Sikora, M., Begelman, M. C., & Rees, M. J. 1994, ApJ, 421, 153

Sikora, M., Blazejowski, M., Moderski, R., & Madejski, G. M. 2002, ApJ, 577, 78

Stawarz, L., & Petrosian, V. 2008, ApJ, 681, 1725

Stecker, F.W., Baring, M. G. & Summerlin, E. J. 2007, ApJL, 667, L29.

Stecker, F.W., & Scully, S.T. 2008, A &A, 478, L1.

Stecker, F.W., & Glashow, S.L. 2001, Astropart. Phys. 16, 97

Tavecchio, F., Maraschi, L., & Ghisellini, G. 1998, ApJ, 509, 608

Tavecchio, F., Ghisellini, G., Ghirlanda, G., Costamante, L., & Franceschini, A. 2009, MNRAS, 399, L59

Urry, C.M., & Padovani, P. 1995, PASP, 107, 803

Zacharopoulou, O., Khangulyan, D., Aharonian, F., & Costamante, L. 2011, ApJ in press

Zirakashvili, V.N., & Aharonian, F. 2007, A&A, 465, 695

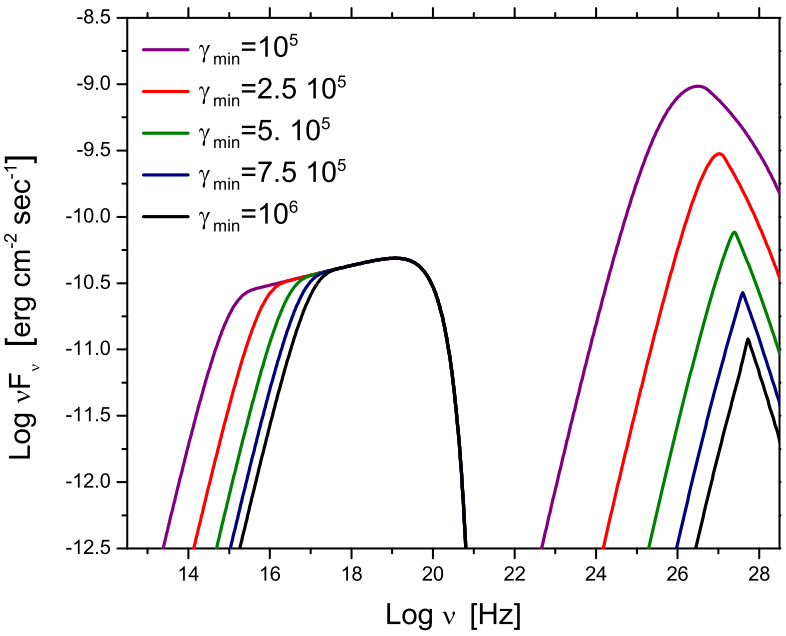

Fig. 1.— Stationary SSC spectra for different values of the low-energy cut-off. Above $\gamma_{\rm min} \sim 3 \times 10^5$ we are very deep in the Klein-Nishina regime and the peak of the Compton emission appears very sharp. As one reduces $\gamma_{\rm min}$, the suppression of the cross-section decreases and the minimum Compton energy drops to lower energies. Thus, the peak of the Compton flux raises significantly, whereas the synchrotron peak remains constant. A Doppler factor $\delta = 50$ has been used for the plot.

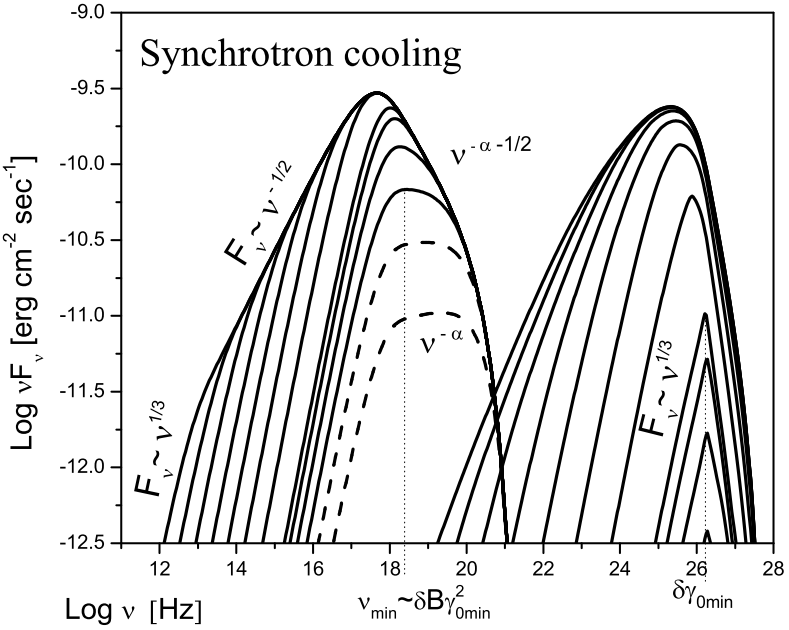

Fig. 2.— Evolution of the observed SSC spectrum for constant injection of a narrow power-law electron distribution, with modifications due to synchrotron cooling taken into account. The magnetic field is $B = 1G$. The hard (1/3) synchrotron and Compton spectral wings are observed for timescales shorter than the cooling timescale of the γ_0-particles, i.e., in the present application for timescales ≤ 0.1 days. The figure shows the expected spectral evolution for a total (observed) time $t \sim 1$ day. Parameters used are $R_0 = 7.5 \times 10^{14}$ cm, $\gamma_{\rm min} = 7 \times 10^4$, $\gamma_{\rm max} = 2 \times 10^6$, power law index $p = 2.85$ and Doppler factor $\delta = 25$. The total injected power is $Q \sim 10^{41}$ erg/sec.

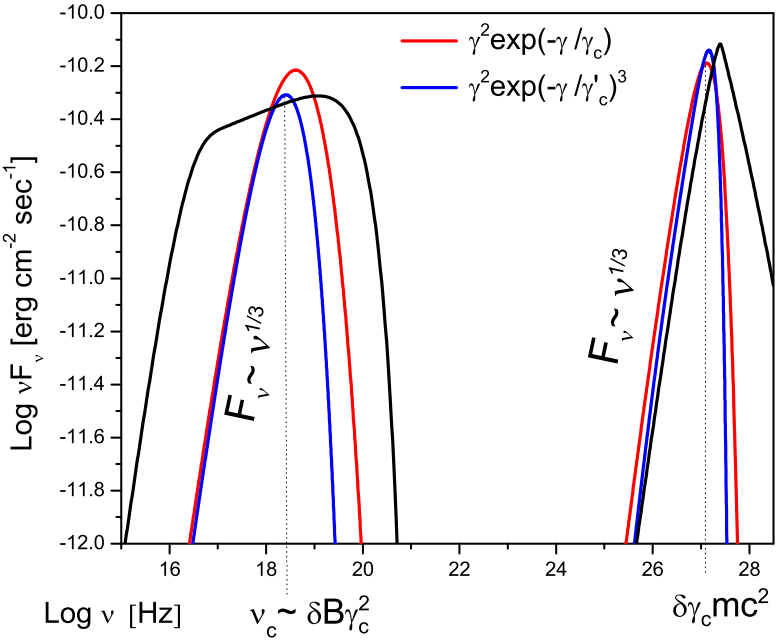

Fig. 3.— SSC modelling with different electron distributions. **Black line:** *Power-law* with large value of the minimum energy (as in Tavecchio et al. 2009). The parameters used are $\gamma_{\rm min} = 5 \times 10^5$, $\gamma_{\rm max} = 4 \times 10^7$, power law index $p = 2.85$, $B = 4 \times 10^{-4}$ G, $k_e = 6.7 \times 10^8$ cm^{-3}, $R = 5.4 \times 10^{16}$ cm and Doppler factor $\delta = 50$. **Red line:** Relativistic *Maxwellian* distribution $N_e = K_e \gamma^2 \exp(-\frac{\gamma}{\gamma_c})$ with parameters $\gamma_c = 1.5 \times 10^5$, $B = 0.07$ G, $K_e = 3 \times 10^{-14}$cm^{-3}, $R = 2 \times 10^{14}$cm and $\delta = 33$. The peak of Compton flux occurs in the KN regime as $(B/B_{cr})\gamma_c^3 \simeq 160 >> 1$. **Blue line:** Relativistic *Maxwellian* distribution $N_e = K_e \gamma^2 \exp(-\frac{\gamma}{\gamma_c})^3$ with parameters $\gamma_c = 5.3 \times 10^5$, $B = 0.06$ G, $K_e = 4 \times 10^{-15}$ cm^{-3}, $R = 2 \times 10^{14}$ cm and $\delta = 33$.

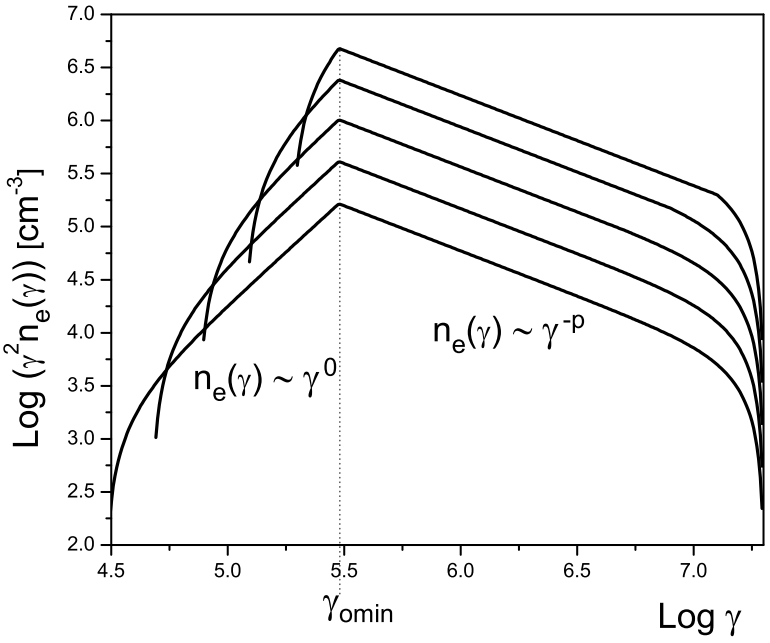

Fig. 4.— Illustration of the evolution of the electron distribution for constant injection and dominant adiabatic losses. The expansion of the source does not modify the power-law index above the initial low-energy cut-off $\gamma_{0,\mathrm{min}}$, whereas below it the distribution becomes approximately flat. The electron number density depends on radius as $n_e \propto R^{-2}$

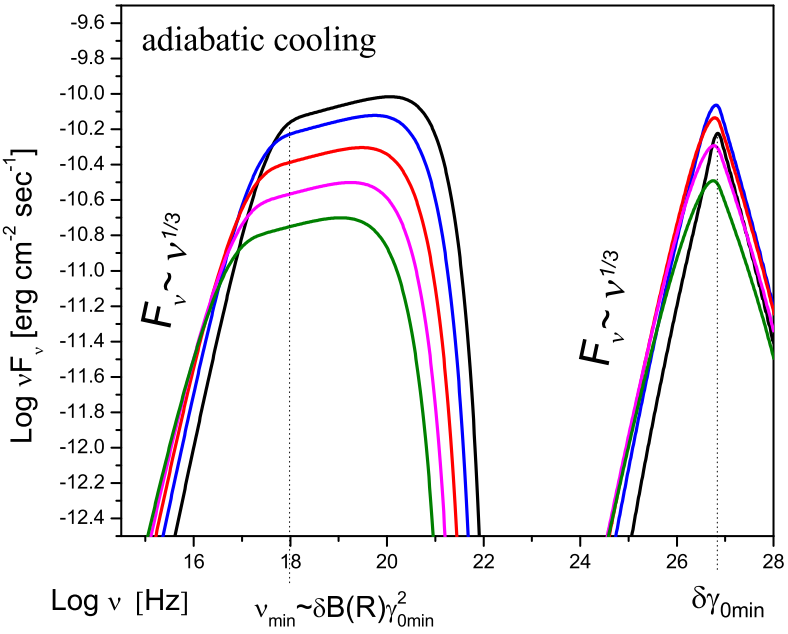

Fig. 5.— Evolution of the observed SSC spectrum with constant injection of a narrow power-law and dominant adiabatic losses. As the source evolves, the synchrotron peak decreases and gets shifted to smaller energies following the decrease of the magnetic field. For the magnetic field, we use an initial value $B_0 = 0.075$ G and we assume that it scales as $B = B_0\ (R_0/R)$ (i.e., $m = 1$). The initial radius is $R_0 = 7.5 \times 10^{14}$ cm, expanding up to $R = 10R_0$ (at $u = 0.1$ c) and corresponding to observed timescales of the order of $t \sim 30/\delta$ days. The total injected power is $Q \sim 5 \times 10^{41}$ erg/sec. Other parameters used are $\gamma_{\rm min} = 3 \times 10^5$, $\gamma_{\rm max} = 2 \times 10^7$, power law index $p_1 = 2.85$, Doppler factor $\delta = 25$ and $Q_0 = 1.5 \times 10^{52}$ sec^{-1}. Note that timescales are comparable to the synchrotron cooling case.

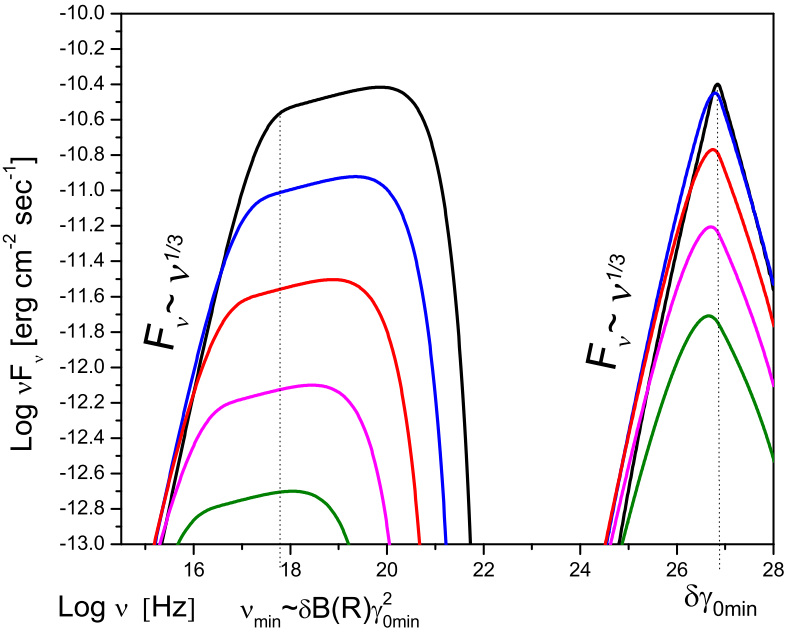

Fig. 6.— Same as Fig. 5 but for a different magnetic field scaling, $m = 2$. Other parameters are the same as in Fig. 5.

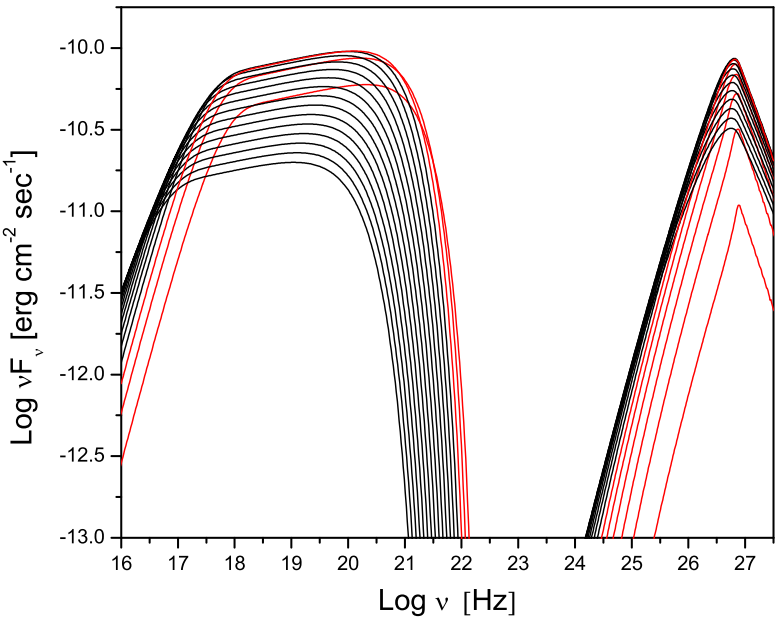

Fig. 7.— Evolution of the SSC spectrum with dominant adiabatic losses (for $B \propto 1/R$, i.e., $m = 1$) from $R_0 = 7.5 \times 10^{14}$ cm to $R = 10R_0$, and corresponding observed luminosities. Whereas the synchrotron peak gets with time significantly shifted to lower energies, the Compton peak can appear almost static. The Compton flux reaches its maximum at a greater radius than for the synchrotron one. Synchrotron and Compton fluxes are shown until maximum (with red lines) and after (with black lines).

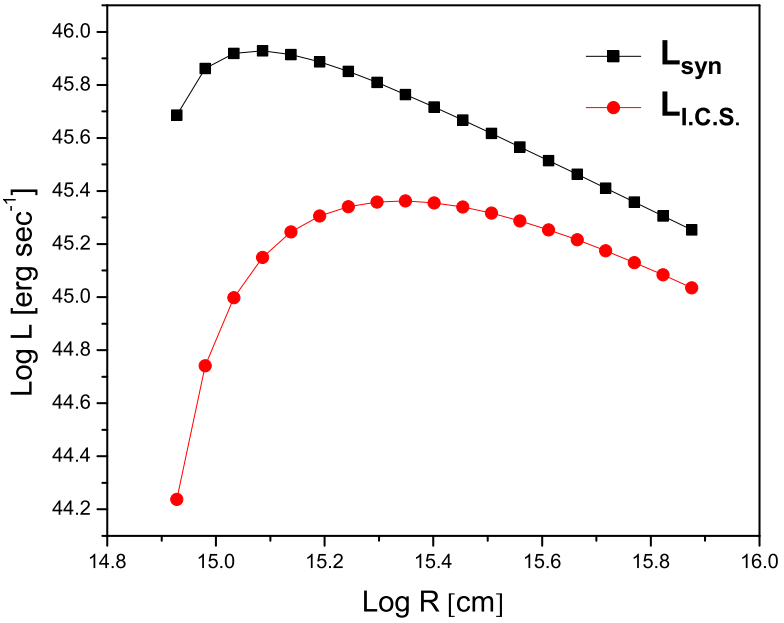

Fig. 8.— Evolution of the SSC spectrum luminosities with dominant adiabatic losses (for $m = 1$), see also Fig. 7. The Compton flux reaches its maximum at greater radius (i.e., later) compared to the synchrotron one. While during the raising phase the variability pattern approximately shows a quadratic behavior, the correlation becomes almost linear during the declining phase.

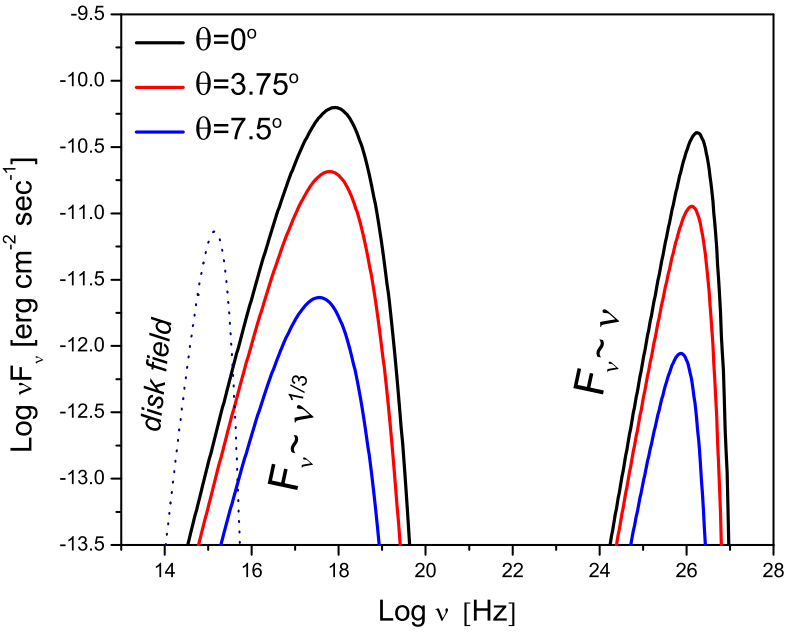

Fig. 9.— External Compton scenario for a Maxwellian-type electron distribution (with $\alpha_p = 0$). The observed spectrum is calculated for different angles θ to the observer. The synchrotron slope follows $F_\nu \propto \nu^{1/3}$. In the TeV range $F_\nu \propto \nu^1$, i.e., harder than in the SSC case. The dashed line corresponds to the assumed disk spectrum. The bulk Lorentz factor of the jet is $\Gamma = 13$ and the peak energy of the electron distribution is $\gamma_c = 2 \times 10^4$. For the disk photon field a temperature $T = 1.75 \times 10^4$ K is assumed. The relevant radius R_d of the disk is considered to be of the same dimension as the jet (10^{15} cm). The magnetic field is $B = 1$ G and a fraction $\xi = 0.1$ of the disk photons is assumed to be rescattered by the BLR.

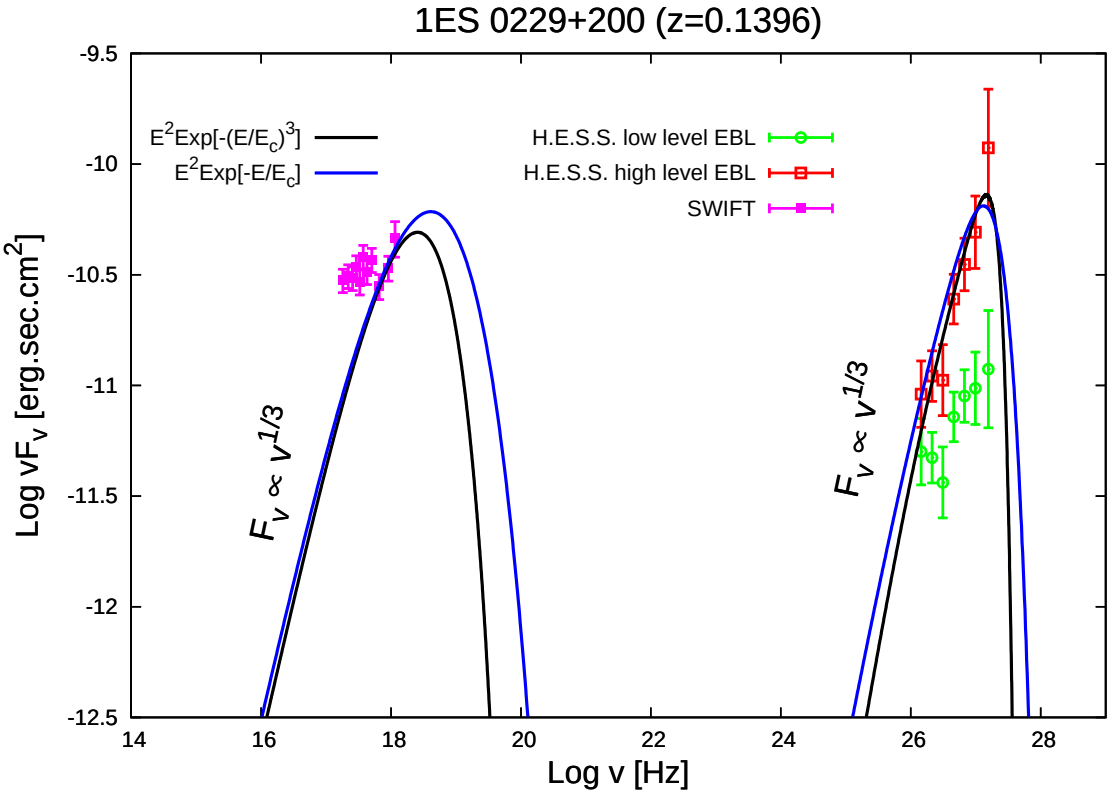

Fig. 10.— The hard spectrum blazar 1ES 0229+200 at z=0.139 with SED modeled within an SSC approach using Maxwellian-type electron distributions. All parameters used are the same as in Fig.3. Data points shown in the figure are from Zacharopoulou et al. (2011), where the intrinsic (de-absorbed) source spectrum has been derived based on the EBL model of Franceschini et al. (2008) with (i) EBL level as in their original paper ("low level EBL") and (ii) (maximum) EBL level scaled up by a factor of 1.6 ("high level EBL").